Composite infrared bolometers with Si_3N_4 micromesh absorbers

P. D. Mauskopf, J. J. Bock, H. Del Castillo, W. L. Holzapfel, and A. E. Lange

We report the design and performance of 300-mK composite bolometers that use micromesh absorbers and support structures patterned from thin films of low-stress silicon nitride. The small geometrical filling factor of the micromesh absorber provides 20× reduction in heat capacity and cosmic ray cross section relative to a solid absorber with no loss in IR-absorption efficiency. The support structure is mechanically robust and has a thermal conductance, $G < 2 \times 10^{-11}$ W/K, which is four times smaller than previously achieved at 300 mK. The temperature rise of the bolometer is measured with a neutron transmutation doped germanium thermistor attached to the absorbing mesh. The dispersion in electrical and thermal parameters of a sample of 12 bolometers optimized for the Sunyaev–Zel'dovich Infrared Experiment is ±7% in $R(T)$, ±5% in optical efficiency, and ±4% in G.

Key words: Infrared bolometers, silicon nitride, micromesh.

1. Introduction

Bolometers are the most sensitive detectors of broadband electromagnetic radiation at wavelengths between 250 μm and 5 mm, a wavelength range that includes most of the energy in the cosmic microwave background. A new generation of balloon-borne and orbital missions (BOOMERanG, MAXIMA, COBRAS/SAMBA) designed to measure structure in the cosmic microwave background requires sensitive bolometric detectors that can be operated with minimum cryogenic complexity. In addition, long-duration balloon experiments conducted above the Antarctic require detectors with a significantly reduced cross section to cosmic rays to offset the enhanced cosmic ray flux near the Earth's poles. We report on improvements in bolometer performance at 300 mK achieved by new methods of detector design and construction that make use of photolithography on thin films of silicon nitride.

The theory of the electrical and thermal characteristics of bolometers has been discussed in detail (see, e.g., Mather[1]). A simple model describes a bolometer as an absorber with heat capacity C connected to a thermal bath at temperature T_c by a thermal conductance G. The temperature of the absorber changes in response to changes in incident power; these temperature fluctuations are typically converted into voltage fluctuations by means of a current-biased thermistor. The detector has an intrinsic time constant given by $\tau_e = \alpha(C/G)$ where α is a constant of order unity. The responsivity of the bolometer to signals modulated at frequency ω is

$$S(\omega) = \mathrm{S}_0 \frac{1}{\sqrt{1 + \omega^2 \tau_e^{\,2}}}, \tag{1}$$

where the dc responsivity, $S_0(V/W)$, depends on the properties of the thermistor and on the thermal conductance, G. The sensitivity of an optimized bolometer to fluctuations in incident power is often expressed as a noise equivalent power (NEP) given by the bolometer noise divided by its responsivity,

$$\mathrm{NEP}_{\mathrm{opt}} = \frac{\gamma}{\eta} \sqrt{4 k_B T_c^{\,2} G}, \tag{2}$$

where γ is of order unity and has a weak dependence on the temperature coefficient of the thermistor, and η is the coupling efficiency of the bolometer to incident optical power. For an optical loading Q on the bolometer, the optimum sensitivity is achieved with $G \simeq Q/T_c$.

P. D. Mauskopf, J. J. Bock, W. L. Holzapfel, and A. E. Lange are with the California Institute of Technology, Mail Stop 59-33, Pasadena, California 91125. H. Del Castillo is with the Jet Propulsion Laboratory, Pasadena, California 91109. J. J. Bock is also with the Jet Propulsion Laboratory.

Received 5 April 1996; revised manuscript received 23 July 1996.
0003-6935/97/040765-07$10.00/0

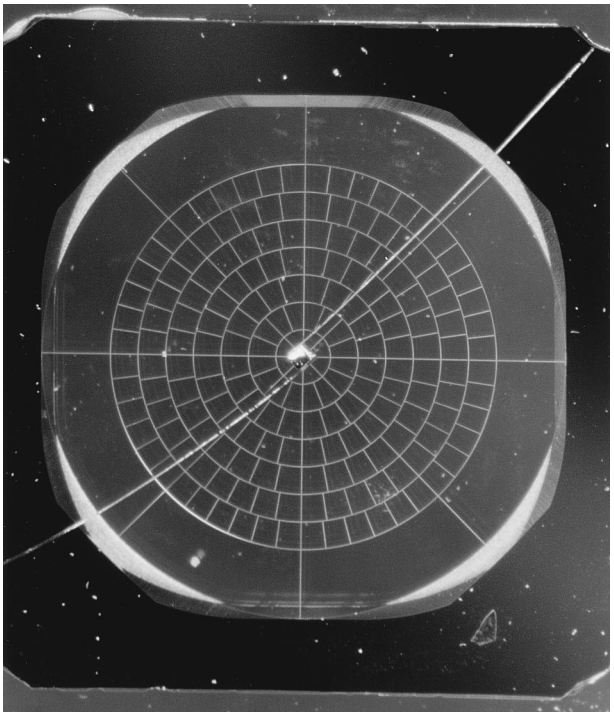

Fig. 1. Photograph of a micromesh bolometer that has been manufactured from a 1-μm-thick membrane of silicon nitride. The absorber is 5.6 mm in diameter, the long radial legs are 1 mm long and 5 μm wide, and the legs in the meshlike absorber region are 200 μm long and 4 μm wide. A metallic film is evaporated onto the absorber to match the impedence of free space. A (250-μm)^3 NTD germanium thermistor is attached to the diamond region at the center and read out with two long Nb-Ti lead wires.

Applications with low optical background loading and rapid modulation require bolometers with minimal thermal conductances and heat capacities. At a given base temperature, properties of the materials used to fabricate the absorber, thermistor, and support structure constrain C and G for a device and thus set a fundamental limit of performance. Spurious sources of energy in the environment such as mechanical vibrations, temperature fluctuations, and cosmic rays may, however, prevent this limit from being realized.

We describe measurements at 300 mK of bolometers that use a new type of absorber and a mechanical support structure consisting of a thin film of metal evaporated on a freestanding mesh of silicon nitride (see Fig. 1). Matched neutron transmutation doped (NTD) germanium thermistors and leads are assembled separately and attached to the absorber with epoxy. This architecture provides (1) a low base thermal conductivity and thus a low NEP, (2) a low intrinsic heat capacity per unit absorbing area, (3) a large absorbing area that allows coupling to a larger throughput and thus to lower frequencies, (4) reduced cosmic ray cross section, and (5) reduced microphonic disturbances. We have fabricated micromesh bolometers with electrical NEP's that range from 2×10^{-17} W/$\sqrt{\text{Hz}}$ to $>3 \times 10^{-16}$ W/$\sqrt{\text{Hz}}$ at 300 mK. These devices have been used for astrophysical observations from the ground [Sunyaev–Zel'dovich Infrared Experiment (SuZIE)] and will be flown on several balloon-borne telescopes (MAXIMA, PRONAOS, BOOMERanG).

2. Thermistor and Leads

The NTD germanium thermistor has a resistance versus temperature dependence given by

$$R(T) = R_0 \exp\left(\sqrt{\frac{\Delta}{T}}\right). \tag{3}$$

The electrical leads and contacts must have low thermal conductivity and low heat capacity. We have previously provided electrical contact to the thermistor via graphite fibers attached to the thermistor with silver epoxy.[2] Over the course of several years of fabrication and testing, we found this lead technology to have several drawbacks. Even small amounts of silver epoxy increased the time constant of detectors owing to silver epoxy's large heat capacity, and the silver epoxy changed the electrical properties of the thermistors because of stress developed at the contact from differential thermal contraction. Attaching the leads to the chip with a minimal amount of silver epoxy was a difficult and time-consuming process with a low yield. Low-frequency contact noise associated with the electrical contact between the silver epoxy and the graphite was often observed and was found to increase over time. In addition, many silver epoxy joints failed after repeated thermal cycling.

To avoid these problems, we have abandoned the use of graphite fiber leads in favor of copper-clad niobium–titanium (Nb–Ti) superconducting wire that is indium-soldered to the germanium thermistor. Niobium–titanium wire has been used as leads for composite bolometers operating below 100 mK[3] and was easily adaptable to higher temperatures, with a critical temperature of 9.26 K. Because the wires superconduct, the electrical resistance is negligible, and the thermal conductivity is dominated by the lattice. Extrapolating from measurements at higher temperatures,[4] we estimate that the thermal conductivity should be 1.5×10^{-11} W/K for a 1-cm lead of 12.5-μm-diameter wire at 300 mK, comparable with the thermal conductivity for the same length of graphite. We measure the combined paralleled thermal conductivity of two Nb–Ti leads, each 5 mm long, to be 7×10^{-11} W/K at 315 mK, in agreement with our estimate.

The Nb–Ti leads are prepared from commercial copper-clad Nb–Ti wire with a core diameter $\geq$6 μm and an outer diameter twice the core size.[5] The wire is wound around a Teflon loom, and the copper cladding is removed from the central 5 mm by masking the ends with wax and immersing the loom in nitric acid. The wax is removed in heated trichloroethane (TCA). Copper has a large heat capacity, so one end of each lead is clipped within 40 μm of the bare Nb–Ti wire and soldered to a gold pad on the germanium thermistor with $\simeq 3.3 \times 10^{-8}$ cm^3 of indium.

With this procedure we obtain a high yield of well-matched thermistors. To determine the electrical and thermal properties of thermistors and leads, we mount them on a temperature-controlled cold stage with a calibrated thermometer. We measure the resistance versus temperature of the thermistor, $R_b(T)$, and the thermal conductivity of the leads, G, using an ac bias readout circuit designed to be stable over hundreds of seconds of integration, similar to the bolometer readout circuit implemented in the Infrared Telescope in Space.[6] This circuit generates a stable ac current with an oscillator and a cold load resistor, $R_L \gg R_b$ in series with the thermistor. The amplitude of the ac voltage across the thermistor is proportional to its resistance. At low-bias currents the temperature of the thermistor is equal to the temperature of the cold stage; but at higher-bias currents the electrical power, P_e, dissipated in the thermistor causes the temperature of the thermistor to rise by P_e/G and its resistance to drop.

Thermistors with indium-soldered Nb–Ti leads showed little or no change in their electrical and thermal properties unless a large amount of indium solder was used. We measured the resistance versus temperature of six thermistors with indium-soldered Nb–Ti leads and different geometries: Three were cubes 255 μm on a side, and three were 200 × 200 × 255-μm rectangular prisms. We found that each set of three thermistors had Δ matched to within 0.3% and R_0 matched to within 3% with no care taken to minimize the amount of indium solder used. Two out of the three thermistors measured in each set had relatively small amounts of indium solder, and their R_0's were matched to better than 0.5%. Finally, one of the thermistors was intentionally fabricated with more than 10 times the amount of indium solder used on the others, and it was seen to have no effect on its measured value for Δ but did raise the value of R_0 by 13%. The indium solder joints display no observable contact noise at frequencies as low as 20 mHz, even with less than 3.3×10^{-8} cm^3 of indium solder.

The resistance of these thermistors at room temperature is dominated by the niobium–titanium, which has a resistivity of 2×10^{-4} Ω cm, which corresponds to a resistance of 40 Ω. The thermistors contribute approximately 10 Ω for a typical resistance of 50 Ω. For the six thermistors described above, we selected Nb–Ti wires with similar lengths of bare Nb–Ti and similar room-temperature resistances. We measured the thermal conductivities of all of the leads at 300 mK to be matched to within 3%.

By observing the step response of the system to a change in current, we measured the heat capacities at 400 mK of 12 thermistors constructed in this manner. For this test, we bias the thermistor and leads with a small square-wave ac current on top of a dc level corresponding to the peak of the load curve, where the dynamic impedence of the thermistor and leads, $Z_{\mathrm{dyn}} = \mathrm{d}V/\mathrm{d}I$, is equal to zero. The ac component of the output voltage across the bolometer exhibits an exponential decay with time constant, τ_e, corresponding to the heating or cooling of the bolometer. During this decay the resistance of the bolometer changes, which also changes the amount of electrical power dissipated in the thermistor in an "electrothermal feedback" that decreases the bolometer response time. The measured electrical time constant, τ_e, is related to the thermal time constant, $\tau = C/G$, by

$$\tau = \tau_e \left[\frac{2GR_b(Z_{\mathrm{dyn}} + R_L)}{(Z_{\mathrm{dyn}} + R_b)(R_b + R_L)} \right]. \tag{4}$$

The heat capacity of the thermistor and leads assembly was measured to be 1.5×10^{-11} J/K at 400 mK.

3. Micromesh Absorber

A critical part of all IR bolometers is the absorber that converts incident IR radiation into heat. Composite bolometers traditionally use a uniform metallic film deposited on a dielectric substrate as a broadband absorber. To obtain frequency-independent absorption, the film must be purely resistive and its impedence in parallel with the admittance of the dielectric film should match the impedence of free space, $Z_0 = 377\ \Omega/\square$. This corresponds to a film resistance of $R_\square = Z_0/(n + 1)$, where n is the index of refraction of the dielectric substrate.[7] Different groups have used a variety of metals, including bismuth[8,9] and gold,[10] for the film. Bismuth is a convenient choice because its low electrical conductivity requires thicknesses of 500 Å to achieve the proper impedence in a solid film. Gold films must be significantly thinner (≃few nm), and at this thickness it is difficult to achieve good film uniformity.

Solid absorbers such as those described above have historically exhibited an anomalously high heat capacity that appears to be associated with surface contamination of the substrate.[2] In principle, it is possible to construct a mesh of lossy wires that achieves good absorption in band as long as the grid constant of the mesh is small relative to a wavelength. We have produced such a mesh absorber structure by patterning a thin film (≃1 μm) of low stress Si_3N_4 that is deposited on a silicon wafer. The geometry of the devices we have produced was inspired by a spider's web and is shown in Fig. 1. After the nitride has been etched, the wafer is diced and placed in a silicon etch, leaving only the mesh of nitride connected by a small number of legs to a solid silicon frame. We then evaporate 50 Å of chromium and 200 Å of gold onto the center region of the absorber through a shadow mask, producing a network of wires.

We have produced freestanding absorbers with a wide variety of geometries (Table 1). In the region active for absorption, the width of the legs is 4 μm, and the grid spacing is as small as 60 μm in some absorbers and as large as 400 μm in others. We have made absorbers with active areas from 5 mm^2 (2.5 mm ϕ) to 24.5 mm^2 (5.6 mm ϕ). The support legs of the absorber are 1 μm thick, 5 μm wide, and 1000 μm long. The filling factor of the absorber is between 2% and 10% of the active area.

Table 1. Spider Web Absorber Geometries[a]

Mask	g (μm)	$2a$ (μm)	ϕ (mm)	FF (%)	l (mm)	s (μm)	N
A	160	4	2.624	5%	1	5	16
B	60	1.5	2.583	5%	1	5	8
C	60	3	2.520	10%	1	5	8
D	60	3	2.520	10%	0.5	2.5	8
E	60	2	2.604	6.7%	1	5	8
F	400	4	5.656	2%	1	5	8
G	400	4	5.656	2%	1	5	16
H	200	3	5.278	3%	1	5	8
I	solid		2.624	100%	1	5	16
J	solid		5.656	100%	1	5	16

g, grid spacing; $2a$, line width in absorber; ϕ, absorber diameter; FF, absorber filling factor; l, support leg length; s, support leg line width; N, number of support legs.

The heat capacity budget of a micromesh bolometer is shown in Table 2. At 300 mK, the heat capacity of the thermistor dominates over that calculated for the absorber by a factor of ≃30. It is therefore difficult to measure the heat capacity of the silicon nitride accurately. To obtain an experimental upper limit, we measured the heat capacity, thermal conductance, and $R(T)$ of thermistors and electrical leads alone. Then we attached a calibrated thermistor to a micromesh absorber and repeated the measurements. We measured the heat capacity of a solid circular film of nitride 2.56 mm in diameter with a layer of evaporated metal with thickness optimized for the spider geometry to be $\leq 4 \times 10^{-11}$ J/K for a heat capacity per geometric area of $\sigma \leq 8$ pJ/mm^2 at 400 mK. Direct measurements of the heat capacities of the largest absorbers, with 3% filling factor and 5.3 mm diameter, give an upper limit of $C_{\text{abs}} \leq 5 \times 10^{-12}$ J/K at 400 mK. From these measurements it is clear that the heat capacity of the absorber is no longer a constraint on the size of IR bolometers. In particular, this architecture allows coupling to radiation with more than 2× the wavelength and 4× the throughput of previous bolometers with no loss of speed or sensitivity.

The thermal conductance properties of the absorber are given in Table 3. The thermal conductivity of the silicon nitride is extrapolated from a measurement at $T \geq 200$ mK assuming a power law in temperature.[11] The conductivity between absorber and heat sink is more than 1 order of magnitude smaller than the thermal conductivity of the nylon supports used in other low-background composite bolometers at 300 mK, which allows micromesh bolometers to achieve higher sensitivity under low-background conditions. The internal thermal conductivity of the absorber, G_{abs}, is equivalent to the conductivity of a single leg in the central

Table 2. Estimated Heat Capacities of Thermistor and Lead Components

Component	C_v Electron (J/cc K^2)	C_v Lattice (J/cc K^4)	Volume (cc)	C (400 mK) (J/K)
Thermistor				
Ge[a]	1.9×10^{-7}	3.0×10^{-6}	1.66×10^{-5}	4.52×10^{-12}
Pd[b]	1.2×10^{-3}	1.1×10^{-5}	2.6×10^{-9}	1.25×10^{-12}
Au[b]	7.3×10^{-5}	4.2×10^{-5}	5.2×10^{-8}	1.65×10^{-12}
Total				7.42×10^{-12}
Electrical Leads				
Cu[b]	9.7×10^{-5}	6.7×10^{-6}	8.75×10^{-8}	3.4×10^{-12}
NbTi[b]	superconducting	4.0×10^{-6}	1.71×10^{-6}	4.5×10^{-13}
In[b]	1.15×10^{-4}(n)	9.58×10^{-5}	1.25×10^{-7}	7.7×10^{-13}
Pb[b]	1.71×10^{-4}(n)	1.2×10^{-4}	2.5×10^{-8}	2.0×10^{-13}
Total				4.82×10^{-12}
Absorber				
Cr[b]	2.03×10^{-4}	1.19×10^{-6}	3.0×10^{-9}	2.4×10^{-13}
Au[b]	7.25×10^{-4}	4.23×10^{-5}	1.2×10^{-8}	3.0×10^{-13}
Si_3N_4[c]	*	*	2.5×10^{-7}	1.0×10^{-14}
Total				5.5×10^{-13}
Heat Capacity of Thermistor + Leads				1.3×10^{-11}

[a]Ref. 17 (Electronic heat capacity estimated assuming a doping density of 4.9×10^{-16}/cc^2).
[b]Ref. 18.
[c]Ref. 19.

Table 3. Thermal Conductance and Web Properties

H Web	300 mK	100 mK
$G_{absorber}$ (W/K)	6.0×10^{-11}	1.4×10^{-11}
$G_{supports}$ (W/K)	$\leq 2 \times 10^{-11}$	$\leq 1.0 \times 10^{-12}$
τ_{therm} (μs)	250	500
G_{ctr}/G_{opt}	0.95	0.99

absorbing region and has contributions from both the metal film and the silicon nitride. The thermal conductivity of the metal is related by the Wiedemann–Franz law to the electrical conductivity required for absorption and dominates over the silicon nitride at lower temperatures ($T < 300$ mK).

The time required for the absorber to thermalize in response to a step increase in optical power is of interest because this determines the ultimate speed of the detector. It scales as $\tau_{therm} = fC_{abs}/G_{abs}$, where f is a factor of order unity. Thermal nonuniformity across the absorber will result in a loss in responsivity owing to energy leaking out to the thermal bath through the radial supports instead of heating the thermistor at the center. We define the effective thermal conductance for power dissipated at the center of the device as G_{ctr}. Power dissipated uniformly throughout the absorbing film produces a different temperature rise at the thermistor and gives a different effective conductance, G_{opt}. The optical responsivity is degraded by the factor G_{ctr}/G_{opt}. If G_{opt} is optimized for a given background loading, a thermally nonuniform device will be less sensitive compared with a thermally uniform device by the factor $\sqrt{G_{ctr}/G_{opt}}$. The ratio G_{ctr}/G_{opt} is independent of the thermal conductance of the electrical leads that thermally link the frame directly to the center of the absorber and is determined by the ratio of the conductance of the supports to the conductance of the absorber. The thermal efficiency may be closely approximated by

$$\epsilon_{th} = G_{ctr}G_{opt} = \frac{1}{1 + \alpha G_{sup}/G_{abs}}; \qquad G_{sup}/G_{abs} \ll 1, \quad (5)$$

where α is a geometry-dependent factor between 0.2 and 0.4. For the devices listed in the thermal conductance table, $\epsilon_{th} \geq 0.75$. The thermal uniformity may readily be improved by reducing the A/l aspect ratio of the supports. A finite-element thermal analysis indicates that the thermalization time of the absorber is <1 ms and that the loss in responsivity owing to thermal nonuniformity is ≤25% as given in Table 3.

The microphonic properties of the absorber are related to its residual stress, Young's modulus, thickness, and radius. The dependence of the spring constant, k (newtons per meter), of solid circular membranes on these parameters has been calculated and confirmed by measurements of low-stress nitride membranes with residual stresses of 430 MPa and Young's modulus values of 230–300 GPa.[12] For typical film stresses of 100–500 MPa, we estimate the fundamental vibration frequency of the above absorbers with 250-μm^3 germanium thermistors to be between 5 and 20 kHz. We drove mechanical vibrations in various bolometers by coupling the mounting rings to a speaker driven by a sine wave from a Wavetek oscillator. We then observed the resonant frequencies of standard composite bolometers and micromesh bolometers with an optical microscope. The fundamental frequency of vibration for a typical composite bolometer with a 4 mm × 4 mm sapphire substrate suspended on 4 nylon strands was 125 Hz. The lowest frequency vibration mode we observed in a micromesh bolometer was an oscillation of one of the Nb–Ti leads at 1.7 kHz.

Table 4. Average Values and Dispersion in Parameters for Ten Micromesh Bolometers

Parameter	Value	Unit	% Disp
T_b	315	mK	
R_0	8.843	Ω	6.31%
Δ	50.388	K	0.75%
G (400 mK)	9.1×10^{-10}	W/K	3.83%
C (400 mK)	1.8×10^{-11}	J/K	11.1%
τ (400 mK)	15.5	ms	14.1%
Voltage Noise	6×10^{-9}	$V/\sqrt{Hz}$	
Responsivity (0 Hz)	7.2×10^{7}	V/W	
NEP (0 Hz)	8.5×10^{-17}	$W/\sqrt{Hz}$	

4. Optical Efficiency

The optical absorptivity of a micromesh absorber depends on the geometry as well as on the impedence of the absorbing metal film. Each micromesh absorber we have produced has characteristic scales corresponding to the grid spacing, g, and line width, a. Therefore these absorbers have high optical efficiency only for radiation with $\lambda \gg g$; and, in the limit of very short wavelength radiation or particles such as cosmic rays, the interaction cross section is equal to the geometric filling factor, $4a/g$.

We used an adaptation of a circuit model of an inductive grid from Ulrich[13] to estimate the single-pass absorption of the micromesh absorber as a function of frequency and the optimum resistance of the metal film. A freestanding lossy grid absorbs radiation with $\lambda \gg g$ with maximum efficiency when

$$\rho \frac{g}{2at} = 189\ \Omega, \quad (6)$$

where ρ is the electrical resistivity of the metal film and t is its thickness. This result can be understood by noting that the edge-to-edge conductance of the grid should be equal to 189 Ω, in analogy with the optimal impedance for a freestanding solid film.[14] The edge-to-edge conductance of the grid is equal to $\rho(g/2at)$, the impedance of a single leg in the grid. Therefore the quantity t/ρ must be made larger by $g/2a$ than that of a solid absorber by increasing either the thickness or the conductivity of the metal film.

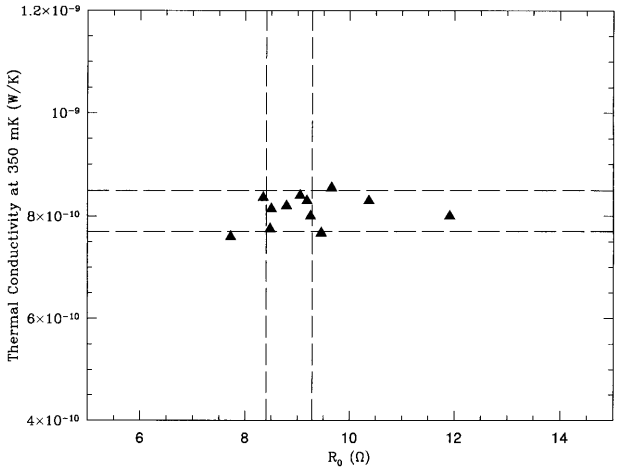

Fig. 2. Distribution of parameters of 12 micromesh bolometers fabricated for the SuZIE instrument. These bolometers are differenced in pairs in an ac bridge circuit and must have parameters matched to within the dashed lines representing ±5% variation. All of these bolometers had Δ matched to within 1%.

For the absorbers we have produced, ≃200 Å of gold is adequate.

We measured the optical efficiency of absorbers with varying geometries and thicknesses of gold placed inside an integrating cavity relative to that of a "standard" composite bolometer with a 4 mm × 4 mm bismuth-coated diamond substrate. We used the SuZIE receiver, which contains an array of six Winston horns that concentrate radiation that enters the cryostat and passes through a cold stop and filter stack designed to transmit radiation in a narrow band centered at either 1.1, 1.4, or 2.1 mm onto bolometers mounted inside integrating cavities. We first determined the relative optical efficiency of each of the six matched channels with a single solid composite bolometer by measuring the optical power looking at 77 or 300-K loads placed in front of the cryostat window. The results for the "standard" bolometer from run to run were reproducible to 5%. The measured value of absorbed power of the micromesh bolometers is a combination of thermal and optical efficiencies and is thus a direct measurement of the bolometers' relative sensitivity to optical power. Micromesh bolometers of type A (Table 1) achieved an efficiency of 75% relative to a bolometer with an equal-area solid substrate and had a detection efficiency (thermal efficiency times optical efficiency) of 60% relative to the "standard" 4 mm × 5 mm substrate bolometer. We measured a detection efficiency of 90–100% for micromesh bolometers of type H relative to 4 mm × 4 mm substrate bolometers at 1.1, 1.4, and 2.1 mm.

5. Device Performance

A distribution of parameters of 12 micromesh bolometers fabricated for the SuZIE receiver is shown in Fig. 2. The SuZIE micromesh bolometers were fabricated with H-style absorbers, 255-μm^3 NTD germanium thermistors, and 21-μm-diameter Nb-Ti wire for the electrical leads. Most of these bolometers satisfied the matching criteria for common mode rejection ratio required for differential radiometry with the SuZIE instrument[15] and five pairs were chosen. These detectors were used during seven nights of observations at the Caltech Submillimeter Observatory in Hawaii; two standard composite bolometers included as a reference were also used. During the run the micromesh bolometers significantly outperformed the old SuZIE bolometers in several areas. First, the micromesh bolometers exhibited reduced sensitivity to mechanical vibrations. Second, they had a higher yield of well-matched detectors, with deviations in physical parameters consistently smaller than 10%. Third, their time constants were ten times smaller than the old SuZIE detectors. Finally, we measured their relative cosmic ray cross section to be approximately 5% of the old style detectors, which was in good agreement with the relative geometrical filling factor.

Because the thermal conductivity of these detectors is dominated by the Nb–Ti wire, lower background detectors were made using smaller-diameter wire. We used 12.5 μm-diameter Nb–Ti wire to produce micromesh bolometers for BOOMERanG, a balloon-borne millimeter-wave telescope, with $G = 1.6 \times 10^{-10}$ W/K, $\mathrm{NEP}_e = 4 \times 10^{-17}$ W/$\sqrt{\mathrm{Hz}}$, and $\tau = 40$ ms.[16] To place a limit on the thermal conductivity of the silcon nitride support structure, we built a bolometer with 6-μm-diameter leads and a measured thermal conductivity of $G = 4 \times 10^{-11}$ W/K. Scaling from the larger diameter wire, we calculate the thermal conductivity of these leads to be at least 2×10^{-11} W/K so that the silicon nitride contributes $G_{\mathrm{support}} \leq 2 \times 10^{-11}$ W/K. This bolometer had a measured $\mathrm{NEP}_e = 2 \times 10^{-17}$ W/$\sqrt{\mathrm{Hz}}$ and a time constant of 180 ms.

6. Conclusions

We have tested silicon nitride micromesh bolometers that have an effective absorptivity equivalent to that of conventional composite bolometers at millimeter wavelengths. The heat capacity of the micromesh bolometer is dominated by the thermistor at 300 mK. The device approaches the behavior of an isothermal absorber under uniform power dissipation.

Micromesh bolometers have several advantages over standard composite bolometers. The heat capacity of a micromesh bolometer is smaller and is dominated by the heat capacity of the thermistor and leads. Larger devices can therefore be manufactured with little cost in heat capacity, which allows coupling to larger throughput with no loss in sensitivity. Further improvements may be realized by reducing the heat capacity of the thermistor and leads. Micromesh bolometers have a small cross section to cosmic rays. Because the silicon nitride supports are mechanically robust and the mass of the absorber is negligible in comparison with the mass of the thermistor, micromesh bolometers have greater immunity to microphonics than do standard composite bolometers. Lower thermal conductance may be

readily achieved by reducing the A/l aspect ratio of the supports. Micromesh bolometers are more easily fabricated than standard composite bolometers and are well suited for use in low-background 2-D arrays.

This research has been made possible by a grant from the Center of Space Microelectronics Technology to the Microdevices Laboratory at Jet Propulsion Laboratory to support the fabrication and development of the micromesh absorbers. The authors also thank P. L. Richards for many useful discussions, W. Holmes for the measurements of the thermal conductivity of silicon nitride, and D. Hebert and the staff at the microlab at University of California, Berkeley, for assistance in manufacturing the original micromesh bolometers. This research has been supported by a NASA Graduate Student Research Program grant to P. D. Mauskopf.

References

1. J. C. Mather, "Bolometers: ultimate sensitivity, optimization, and amplifier coupling," Appl. Opt. **23,** 584–588 (1984).
2. D. C. Alsop, C. Inman, A. E. Lange, and T. Wilbanks, "Design and construction of high-sensitivity infrared bolometers for operation at 300 mK," Appl. Opt. **31,** 6610–6615 (1992).
3. M. Dragovan, University of Chicago, Chicago, Ill. 60637 (personal communication, 1993).
4. E. I. Dyachkov, R. Herzog, I. S. Khukhareva, and A. Nichitiu, "Thermal conductivity and electrical resistivity of Nb–Ti (HT-50) as a function of temperature and magnetic field," Cryogenics **21,** 47–51 (1981).
5. 0.0005″–0.003″ OD copper clad Nb–Ti wire, California Fine Wire Company, Grover City, Calif.
6. M. Devlin, A. E. Lange, T. M. Wilbanks, and S. Sato, "A dc-coupled, high sensitivity bolometric detector system for the infrared telescope in space," IEEE Trans. Nucl. Sci. **40,** 162–165 (1993).
7. J. Clarke, G. I. Hoffer, P. L. Richards, and N. H. Yeh, "Superconductive bolometers for submillimeter wavelengths," J. Appl. Phys. **48,** 4865–4879 (1977).
8. P. M. Downey, A. D. Jeffries, S. S. Meyer, R. Weiss, F. J. Bachner, J. P. Donnelley, W. T. Lindley, R. W. Mountain, and D. J. Silversmith, "Monolithic silicon bolometers," Appl. Opt. **23,** 910–914 (1984).
9. N. S. Nishioka, P. L. Richards, and D. P. Woody, "Composite bolometers for submillimeter wavelengths," Appl. Opt. **17,** 1562–1567 (1978).
10. M. Dragovan and S. H. Moseley, "Gold absorbing film for a composite bolometer," Appl. Opt. **23,** 654–656 (1984).
11. W. H. Holmes, Department of Physics, University of California, Berkeley, Calif. 24720 (personal communication, 1994).
12. S. Hong, T. P. Weihs, J. C. Bravman, and W. D. Nix, "Measuring stiffness and residual stresses of silicon nitride thin films," J. Electron. Mater. **19,** 903–909 (1990).
13. R. Ulrich, "Far-infrared properties of metallic mesh and its complementary structure," Infrared Phys. **7,** 37–55 (1967).
14. G. Hoffer, "Superconducting junction bolometers," Ph.D. dissertation (University of California at Berkeley, Berkeley, Calif., 1980).
15. E. N. Glezer, A. E. Lange, and T. M. Wilbanks, "Bolometric detectors: optimization for differential radiometers," Appl. Opt. **31,** 7214–7218 (1992).
16. J. J. Bock, D. Chen, P. D. Mauskopf, and A. E. Lange, "A novel bolometer for infrared and millimeter-wave astrophysics," Space Sci. Rev. **74,** 229–235 (1995).
17. P. H. Keesom and G. Seidel, "Specific heat of germanium and silicon at low temperatures," Phys. Rev. **133,** 33–39 (1959).
18. R. J. Corruccini and J. J. Gneiwek, "Specific heat and enthalpy of some solids at low temperatures," National Bureau of Standards Monograph 21 (U.S. National Bureau of Standards, Washington, D.C., 1960).
19. V. I. Koshchenko and Y. Kh. Grinberg, "Thermodynamic properties of Si_3N_4," Neorgan. Mater. **18,** 1064–1066 (1982).